International Journal of ChemTech Research
CODEN (USA): IJCRGG, ISSN: 0974-4290, ISSN(Online):2455-9555
Vol.12 No.03, pp 159-168, 2019

Quantum Study of Synthesized 4-(Pyridin-2yl)-N-P-TolylPiperazine-1-Carboxamide as Corrosion inhibitor for Mild steel in Acidic medium

Sumathi.P*[1]

[1]Department of Chemistry, Knowledge Institute of Technology, Salem, Tamilnadu, India

Abstract : Corrosion inhibition of mild steel in 1 M HCl was investigated in the absence and presence 4-(pyridin-2yl)-N-p-tolylpiperazine-1-carboxamide (PTC) has been characterized using LC-MS. Simultaneous thermogravimetry and differential scanning calorimetry (TG-DSC), were used to characterize and to study the thermal behaviour of PTC. The results led to information about thermal stability and thermal decomposition of PTC. The UV-visible absorption spectra indicate the formation of a PTC-Fe complex. Surface analysis by AFM and XRD confirmed the formation of protective coating on the mild steel surface. Quantum chemical calculation were also performed using density functional theory. The quantum chemical parameters such as E_{HOMO} (highest occupied molecular orbital energy), E_{LUMO} (lowest unoccupied molecular orbital energy), energy gap (ΔE), dipole moment (μ), absolute electronegativity (χ), global electrophilicity (ω), polarizability and hyperpolarizability were obtained for the PTC to predict their activity towards metal surface.
Keywords: TG-DSC, UV-visible, DFT, HCl, Mild steel, corrosion.

Introduction

Corrosion of metals is a major industrial problem that has attracted much investigations and researches. Corrosion inhibitors are of considerable practical importance, Mild steel is used widely in engineering for its low cost and good mechanical property, as they are extensively employed in reducing metallic waste during production and in minimizing the risk of material failure, both of which can result in the sudden shut-down of industrial processes, which in turn leads to added costs [1]. The inhibition investigation of dissolution processes by organic substances has been the subject of several researches [2-3]. The results of these studies confirm that the inhibition effect principally depends to adsorptions centers of inhibitory molecules which heteroatoms and aromatic rings in their structure [5-6]. In many cases organic inhibitors (chemically synthesized) were found very efficient but its toxicity and synthesis cost motivated people to develop environment friendly and cheap inhibitors. On the other hand, the obtained data show that these inhibitors act by adsorption on the surface of the metal/solution interface. This process can be done via: (i) electrostatic attraction between the charged metal and the charged inhibitor molecules, (ii) π electrons-interaction with the metal, and (iii) combination of all of the above [7].

DOI= http://dx.doi.org/10.20902/IJCTR.2019.120323

This study deals with investigating the inhibition effect of a new synthesized inhibitor, 4-(pyridin-2yl)-N-p-tolylpiperazine-1-carboxamide (PTC), on the corrosion behavior of mild steel in 1.0 M HCl solution. The study was carried out using UV-visible absorption spectra. Density functional theory was used to calculate some quantum chemical parameters for the corrosion system which allow determining the suitable for the inhibitor to bond with mild steel surface and discussed. Quantum chemical methods have already proven to be very useful in determination of the molecular structure as well as elucidating the electronic structure and reactivity. The X-Ray diffraction patterns (XRD) and atomic force microscopy (AFM) were performed and discussed for surface study of uninhibited and inhibited mild steel samples.

Result and Discussion

Characterization

Lc-ms/ms analysis

Figures 1 show the LC-mass confirmed the purity of PTC. While figure 2 shows the mass spectrum of PTC. A sharp peak at 297.06 m/e was observed which is closely related to the molecular weight of PTC.

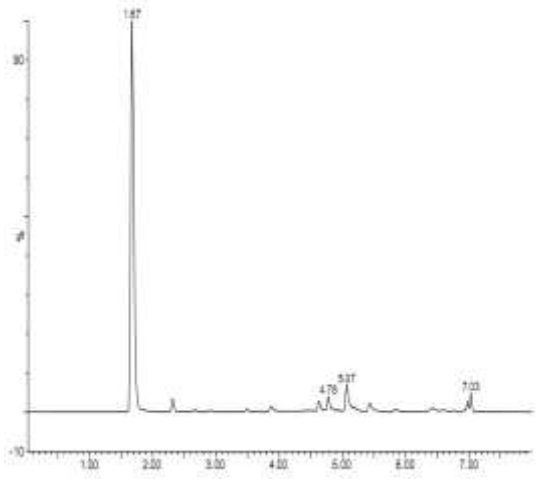

Figure 1 LC Mass spectrum of PTC

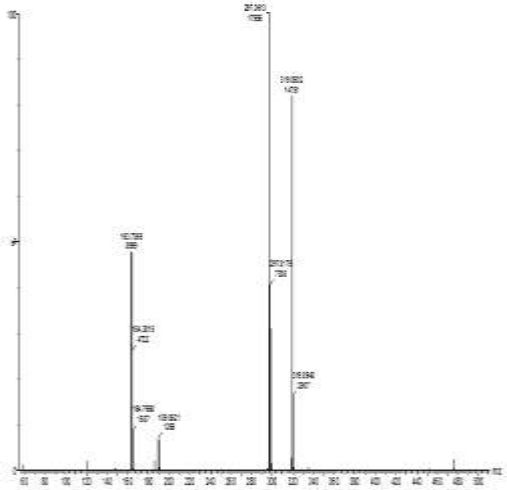

Figure 2 Mass spectrum of PTC

Thermal analysis

TGA and DSC analysis of PTC

From the TG-DSC analysis of PTC exhibiting a simple melt, and the data from PTC is presented in Figure 3 which shows an overlay of the DSC and TGA data in which the TGA curve shows that the thermal decomposition of PTC occurs at 295.3°C with the TG % of ~0.40%. In the DSC curve, endothermic peaks occur at 597.2°C corresponding to fusion and decomposition processes of the compound PTC. This peak is caused by the decomposition of the compound PTC. The presence of an endothermic peak shows the desorption of water molecules from the PTC. The exothermic peak at 192.4 °C corresponds to the crystallization of PTC.

Adsorption Factors

The values of $\Delta G°_{ads}$ was calculated using equation 3.5 and the value at 303K was found to be -23.54 KJ/mol. The higher values of K_{ads} and negative sign of $\Delta G°_{ads}$ indicates that the PTC is strongly adsorbed on the surface of the mild steel. From the table 1, it can be seen that the PTC shows $\Delta G°_{ads}$ values are less negative than -40 KJ/mol at all temperatures, so it can be seen that physical adsorption contributes to the higher percentage of adsorption of PTC on the mild steel surface. The value of K_{ads} and ΔG decreases with increasing in temperature.

$$\Delta G_{ads} = -RT\ln(55.5K_{ads}) \qquad 3.5$$

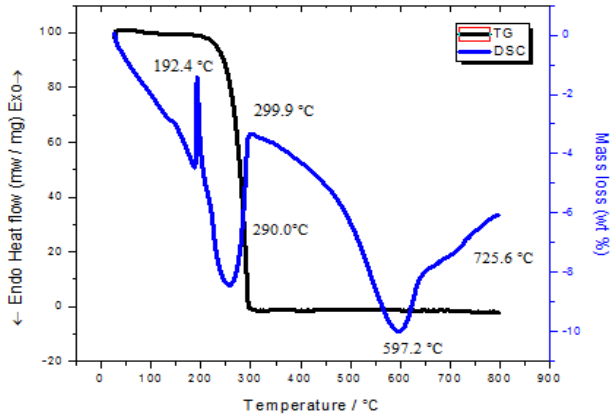

Figure 3 TGA and DSC analysis of PTC

Table 1 Adsorption factors in the presence of PTC on mild steel in 1M HCl at different temperatures

Temperature (K)	R^2	slope	Kads	-ΔG
303	0.9999	1.149	5171	23.54
313	0.9987	1.123	4383	22.82
323	0.9986	1.117	2028	21.95
333	0.9913	1.132	1087	20.75

UV-Visible spectroscopy

UV-Visible absorption spectra the addition of PTC are showed in Figure 4. The corrosion inhibition of mild steel in 1M HC1 in the presence of PTC may due to the formation of thin film on the metal surface by absorption studies in the region 200-400 nm. This observation reveals that the change in surface characteristic is due to the corrosion of mild steel. After corrosion, it can be observed that, in the presence of PTC corresponding to six absorption peaks observed at the same time, The concentration (100 ppm-900 ppm) of PTC of increases with increase in absorbance value 0.5 cm^{-1} shifts to 3.6 cm^{-1}. It is clearly seen that the π-π^* transition of double bond suggesting the interaction between PTC and Fe^{2+} ions in the solution (8).

This indicates that the nitrogen and oxygen groups are tightly held up in the complex with iron. This changes of adsorption peaks clearly indicates that the strong binding between the inhibitor molecules and the ions in the metal surface. These experimental findings provide a strong evidence for the formation of complex between MSPP and Fe^{2+} UV-visible observation confirms the formation of a protective film of metal inhibitor complex on the metal surface.

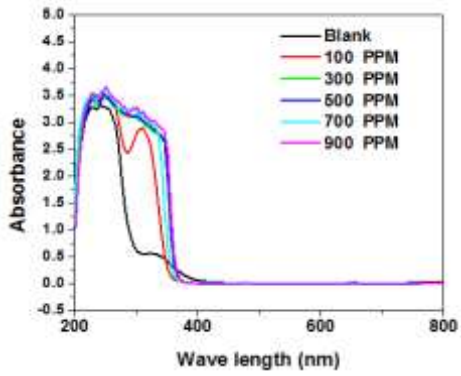

Figure 4 UV-Visible spectra of mild steel in 1M HCl in the absence and presence of PTC

X-Ray diffraction patterns

X-ray diffraction studies were used to determine corrosion products films formed on the surface of mild steel immersed in 1 M HCl in the absence and presence of optimum concentration of the studied PTC (900ppm) .The peak at 2θ = 44.71°, 65.04° and 82.34° in Figure 5 suggested the presence of iron oxide (Fe_2O_3) and very small amount of brown film, which led to corrosion. The peak at 2θ = 44.59°, 57.21° and 64.88° in Figure 6 suggested the absence of oxides iron (Fe_2O_3, Fe_3O_4 and FeOOH). The formation of adsorbed protective film on the surface of mild steel in the presence of PTC is clearly reflected from these observations. No brown film was observed.

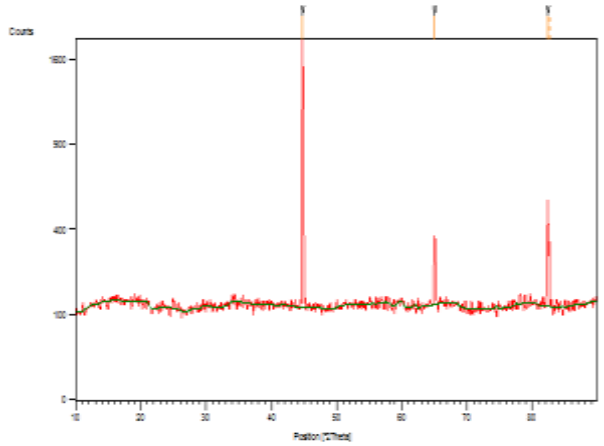

Figure 5 XRD spectrum of mild steel in 1M HCl without PTC

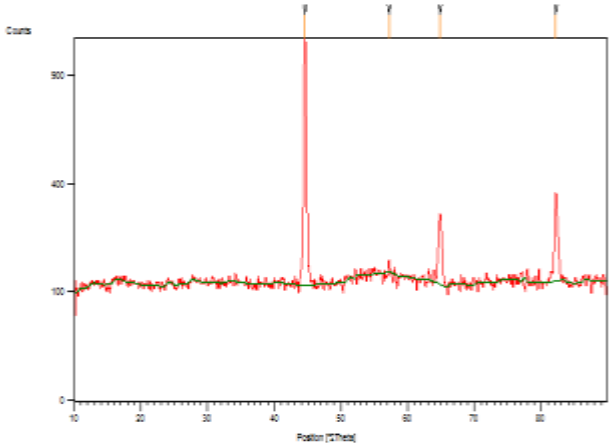

Figure 6 XRD spectrum of mild steel in 1M HCl with PTC

Atomic force microscopy (AFM)

AFM is a powerful tool to investigate the surface morphology and it is very useful to determine the film formation on metal surface in corrosion inhibition studies. AFM images of mild steel in 1 M HCl with and without PTC. The 2D and 3D AFM images were taken at room temperature in the first position range of 0.05 µm to 0.65 µm, and the average roughness of blank mild steel surface and second position range respectively is 0.05 µm to 0.90 µm in absence of inhibitor for 1 M HCl solution as shown in Figure 7. The cracks on the mild steel surface due to acid attack are clearly evident in the photograph. However, in presence of optimum concentration of PTC 900 ppm the average roughness is reduced to first position from 0.025 µm to 0.2 µm, and second position 0.01 µm to 0.19 µm respectively in Figure 8. The smoothness of the surface is due to the formation of a compact protective film of Fe^{2+} to form Fe-PTC on the metal surface there by inhibiting the corrosion of mild steel (9). AFM data for root mean square roughness, average roughness, Maximum peak height and Maximum surface height is given in table 2.

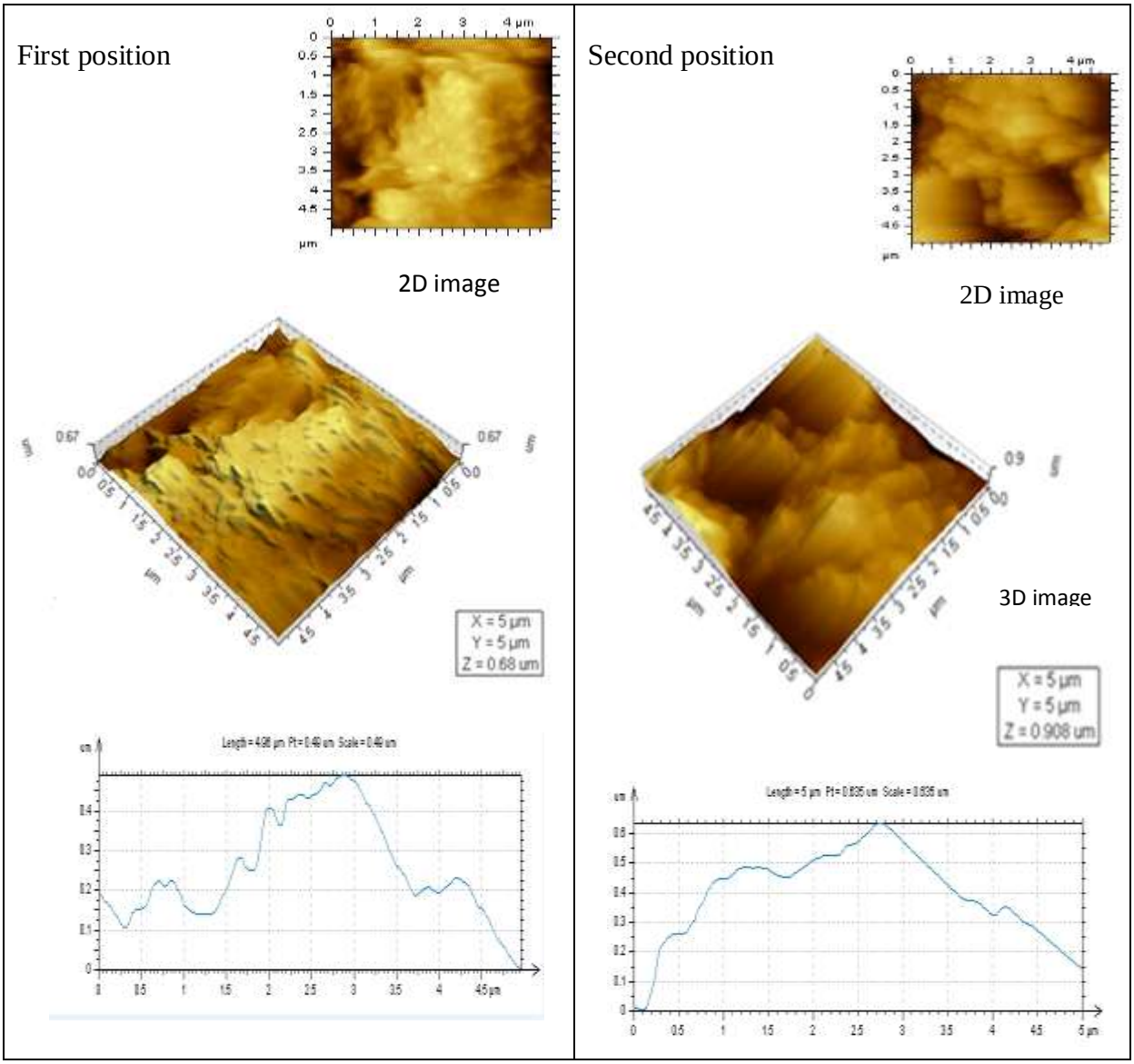

Figure 7 2D and 3D AFM images of mild steel immersion in 1M HCl Without PTC

Table 2 AFM parameters data for mild steel in the absence and presence of an optimum Concentration 900 ppm of PTC in 1M HCl

Sample	Root mean Square roughness (µm)	Average roughness (µm)	Maximum peak height (µm)	Maximum surface height (µm)
1M HCl without PTC (1st position)	0.1290	0.107	0.305	0.680
1M HCl with PTC (1st position)	0.0276	0.022	0.083	0.167
1M HCl without PTC (2nd position)	0.1260	0.099	0.494	0.908
1M HCl with PTC (2nd position)	0.0300	0.024	0.093	0.169

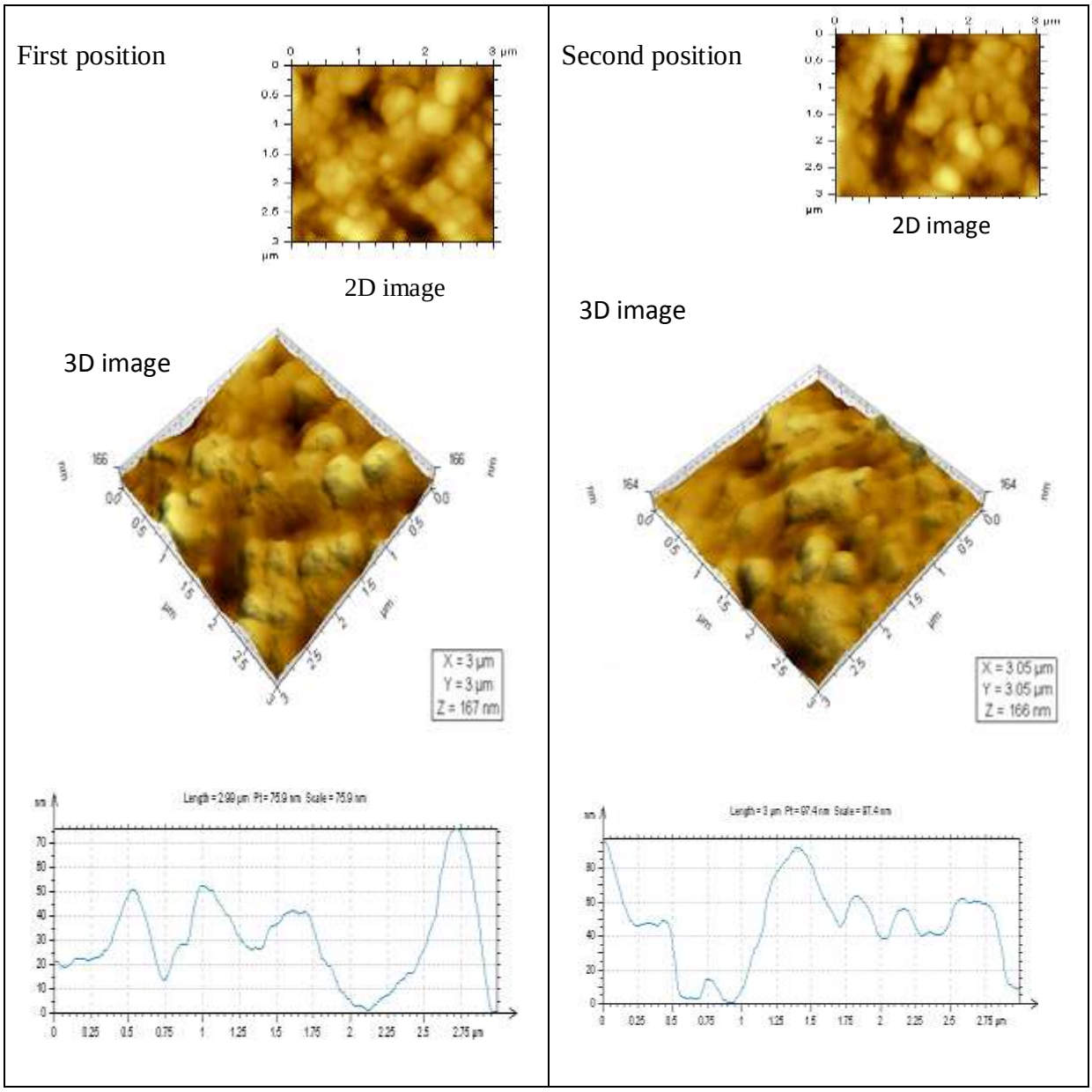

Figure 8 2D and 3D AFM images of mild steel immersion in 1M HCl with PTC

Quantum chemical calculations

Density functional theory (DFT) has been used to analyze the characteristic of the inhibitor / surface mechanism to describe the structural nature of the inhibitor in the corrosion process. Further, DFT is considered as a very useful technique to probe the inhibitor / surface interaction as well as to analyze the experimental data. The quantum chemical parameters such as E_{HOMO}, E_{LUMO}, the energy gap (ΔE), dipole moment (μ), absolute electronegativity (χ), global electrophilicity (ω), polarizability and hyperpolarizability (table 3) were obtained for the PTC to predict their activity towards metal surface. These quantum chemical parameters were generated after geometric optimization with respect to all nuclear coordinates. Optimized molecular structure, HOMO, LUMO are shown in figures 9, 10, 11.

The reactivity of a chemical species can be defined in terms of frontier orbitals HOMO and the LUMO (10). According to frontier molecular orbital theory (FMO), theory of chemical reactivity the formation of a transition state is due to interaction between the HOMO and LUMO of reacting species, the reaction of reactants mainly occurred on the highest occupied molecular orbital (HOMO) and lowest occupied molecular orbital (LUMO). The energy of HOMO (E_{HOMO}) is related to ionization potential while the energy of LUMO

(E_{LUMO}) is directly related to electron affinity. Higher values of E_{HOMO} indicates a tendency of the inhibitor molecule to donate electron to appropriate acceptor molecule with lower energy or 3d orbital of Fe to form coordinate bond. Lower values of $E_{LUMO,}$ the stronger the electron accepting ability of the inhibitor molecule, so that back-donating bond can be formed with its anti-bonding orbital. The more negatively charged heteroatom is the more it can be adsorbed on the metal surface through the donor-acceptor type reaction (11). The smaller the orbital energy gap (ΔE) between the participating HOMO and LUMO, the stronger are the interaction between the two reacting species (13).

The energy gap between HOMO and LUMO is important parameters to determine the theoretical inhibition efficiency. The energy gap is related to softness and hardness. The smaller value ΔE gap means the more reactivity between and higher inhibition efficiency of inhibitors (12). The inhibitors were found to the metal surface and thus form inhibition adsorption layer corrosion. In addition, the electronegativity parameters (χ) are related to the chemical potential and higher value of (χ) indicates better.

Moreover, unoccupied d orbitals of Fe atom can accept electrons from the inhibitor molecule to form a co-ordinate bond while the inhibitor molecule can accept electrons from Fe atom with its anti-bonding orbitals to form back-donating bond (13). In the present study PTC has higher σ value (6.27018) and lower η value (0.15948). Normally, the inhibitor with the least value of global hardness η and highest value of global softness σ is expected to have the highest inhibition efficiency. The increasing values of μ given in table may facilitate adsorption (and therefore inhibition) by influencing the transport process through the adsorbed layer.

Molecular electrostatic potential (MEP) was calculated for PTC optimized structures as shown in Figure 12. Molecular electrostatic potential (MEP) is a plot of static potential mapped on to the constant electron density surface and is a very useful descriptor in understanding the reactive sites of a molecule (14). In the present study the MEP was calculated at the B3LYP/6-311G (d,p) optimized geometry. The MEP also displays molecular size, shape as well as positive, negative and neutral electrostatic potential region in terms of color grading and is very useful in research of molecular structure with its physiochemical property relationship. In PTC structures the negative charge density is localized on the oxygen atoms and nitrogen atoms of the PTC indicating a high ability in metal co-ordination.

The non-linear optical (NLO) parameters such as dipole moment (1.7426), polarizability, anisotropy of polarizability and first order hyperpolarizability of selected compound were calculated using B3LYP level with 6-311G (d, p) basis set and semi empirical (PM6) method. The numerical values of the above mentioned parameters in the presence of an external field (E), the energy of the system is a function of the electric field. First hyperpolarizability is a third-rank tensor that can be described by a 3 X 3 X 3 matrix. The 27 components of the 3D matrix can be reduced to 10 components due to the Kleinman symmetry. The components of hyper polarizability are defined as the coefficients in the Taylor series expansion of energy in an external electric field. Theoretical dipole moment, molecular polarizability and hyper polarizability of PTC are shown in Tables 4.

Urea is one of the prototypical molecules used in the study of the NLO properties of molecular structure. Therefore, it is used frequently as a threshold values for comparative purposes. (μ, α and β of urea are 1.3732 Debye, $3.8351x10^{-24}$ esu and $3.7347xl0^{-31}$ esu respectively). More active NLO properties are predicted for molecules having greater dipole moment, molecular polarizability and hyper polarizability than urea. The dipole moment, polarizability and hyperpolarizability of PTC are greater than those of urea. This hyperpolarizability value is about 8.58 times greater than those of urea. Therefore this PTC can be used as an effective NLO material.

Table 3 Quantum chemical parameters for the PTC

Inhibitor	E Homo (ev)	E Lumo (ev)	ΔE (ev)	Hardness (η)	softness (σ)	χ	ω
PTC	-0.31844	0.00053	0.31897	0.15948	6.27018	0.1589	9.5205
Theoretical dipole moment data of compound							
Inhibitor	μ_x (D)		μ_y (D)	μ_z (D)		μ_{tot} (D)	
PTC	-0.7550		-1.5705	-0.0172		1.7426	

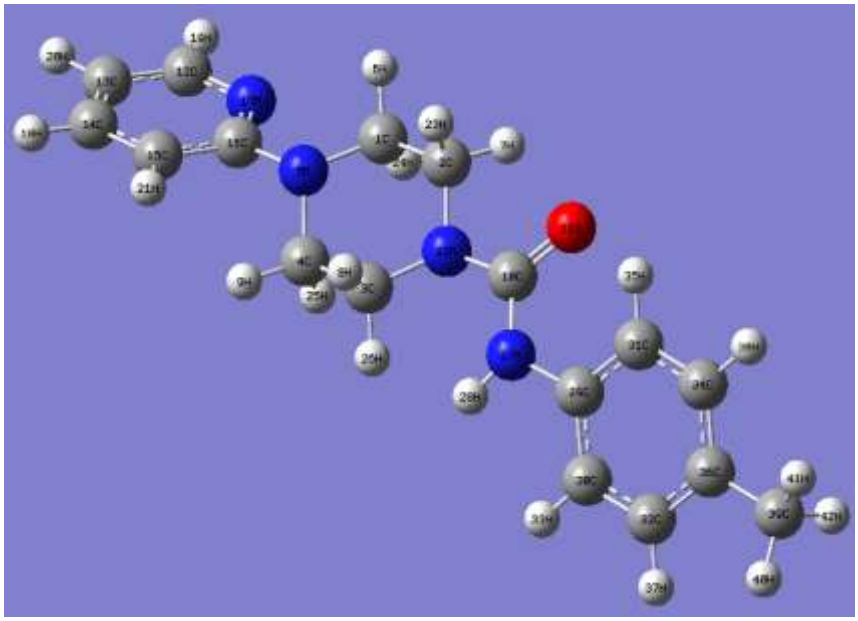

Figure 9 Optimized molecular structure of PTC

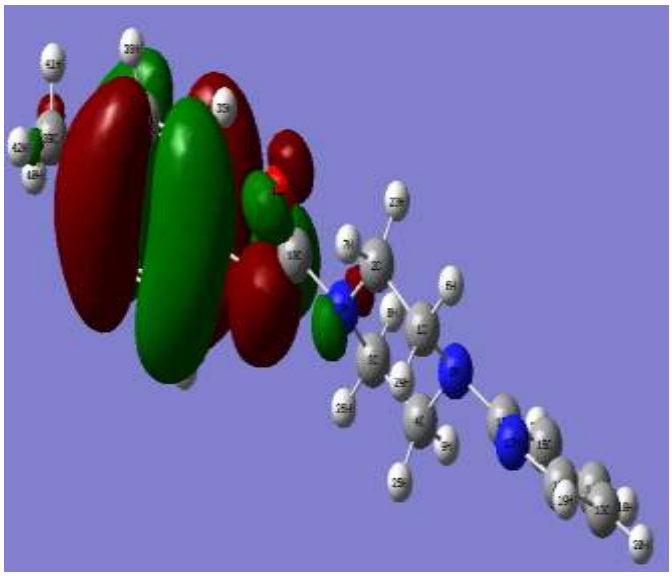

Figure 10 HOMO Surface for PTC molecule

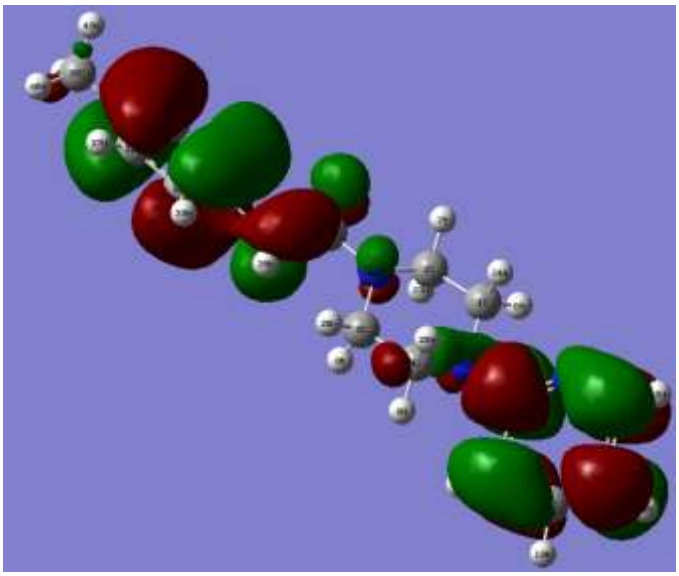

Figure 11 LUMO Surface for PTC molecule

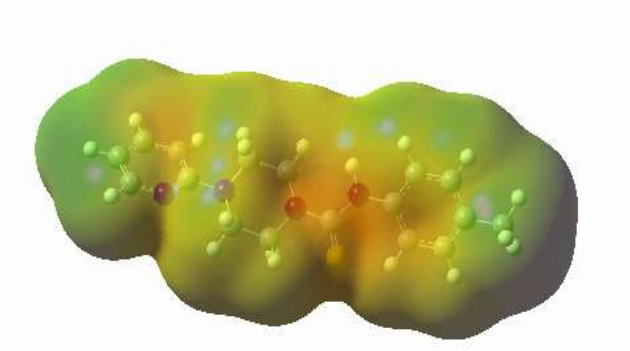

Figure 12 Molecular electrostatic potential map (MEP) of PTC molecule

Table 4 Theoretical polarizability and Hyperpolarizability data of PTC

polarizability (PTC)		Hyperpolarizability (PTC)	
α_{tot} **(e.s.u)**	2.6680×10^{-23}	β_{tot} **(e.s.u)**	3.2066×10^{-30}

Mulliken atomic charges and Fukui functions

The mulliken atomic charge calculation has an important role in the application of quantum chemical calculation to the molecular system. Owing to the effect of dipole moment, polarizability, hyperpolarizability and electronic structure and many properties of the molecular system. Mulliken charges were also used to describe the electronegativity process and transfer of charges in a chemical reaction. In addition, to that mulliken charges are used to analyse the adsorption centre of inhibitor, and it was calculated using B3LYP/6-311G (d, p) method. The Mulliken charge of PTC is shown in Table 5. It has been reported that as the Mulliken charges of the adsorbed center become more negative, the atom more easily donates its electron to the unoccupied orbital of the metal (15). It is clear that the oxygen atom, as well as some nitrogen atoms carries negative charge centers which could offer electrons to the mild steel surface to form a coordinate bond.

Examination of these results shows that all the hetero atoms and some carbon atoms have the negative charges with a high electron density. These atoms thus behave as nucleophilic centers when they interact with the mild steel surface. Therefore, PTC can also accept electrons from Fe through these atoms. It has been reported that excellent corrosion inhibitors can not only offer electrons to unoccupied orbitals of the metal but also accept free electrons from the metal.

Table 5 Mulliken atomic charges for PTC

Atom No	Mulliken charge	Atom No	Mulliken charge	Atom No	Mulliken charge	Atom No	Mulliken charge
1 C	0.204383	**11 O**	**-0.849386**	21 H	0.136883	32 C	-0.087052
2 C	0.225717	12 C	0.076111	**22 N**	**-0.946587**	33 H	0.112941
3 C	0.24195	13 C	-0.341688	23 H	-0.008353	34 C	-0.030415
4 C	0.222809	14 C	0.132	24 H	-0.004223	35 H	0.174642
5 N	**-0.70997**	15 C	-0.38025	25 H	-0.023043	36 C	-0.109656
6 H	0.049978	16 C	0.571452	26 H	-0.000791	37 H	0.11662
7 H	0.063709	**17 N**	**-0.367743**	**27 N**	**-1.144538**	38 H	0.12109
8 H	-0.012374	18 H	0.126035	28 H	0.223259	39 C	-0.023822
9 H	0.025978	19 H	0.146682	29 C	0.522712	40 H	0.032352
10 C	1.733625	20 H	0.159522	30 C	-0.214632	41 H	0.033466
				31 C	-0.223466	42 H	0.024051

Conclusions

The TGA and DSC provided previously unreported information about the thermal stability and thermal decomposition of these compounds. Results obtained from XRD, AFM and adsorption isotherm analyses showed that the mechanism of corrosion inhibition is occur ring mainly through an adsorption process. The results of calculations of B3LYP/6-311G (d, p) shown that the new 4-(pyridin-2yl)-N-p-tolylpiperazine-1-carboxamide (PTC) have good inhibition behavior toward corrosion, the parameters of E_{HOMO}, E_{LUMO}, ΔE, Mulliken atomic charges, dipole moment (μ), polarizability, Hyperpolarizability and fraction of electron transferred from inhibitor molecules to the metallic atoms helped to predict ability of corrosion inhibition, reactivity of PTC toward corrosion inhibition. Through DFT quantum chemical calculations, a correlation

between parameters related to the electronic structure of PTC and their ability to inhibit the corrosion process could be established. PTC purity confirmed by LC-mass.

References

1. Roberge PR. Handbook of Corrosion Engineering; McGraw-Hill Professional Publishing:New York, NY, USA., 1999, 1-3.
2. Zeng L, Zhang GA, Guo XP, Chai CW. Inhibition effect of thioureidoimidazoline inhibitor for the flow accelerated corrosion of an elbow. Corros Sci., 2015, 90: 202-215.
3. Hany M, Abd El-Lateef. Experimental and computational investigation on the corrosion inhibition characteristics of mild steel by some novel synthesized imines in hydrochloric acid solutions. Corros Sci., 2015, 92: 104-117.
4. Hegazy MA, El-Tabei AS, Bedair AH, Sadeq MA. An investigation of three novel nonionic surfactants as corrosion inhibitor for carbon steel in 0.5 M H_2SO_4. Corros Sci., 2012, 54: 219-230.
5. Sherif EM. Corrosion inhibition in 2.0 M sulfuric acid solutions of high strength maraging steel by aminophenyl tetrazole as a corrosion inhibitor. Appl Surf Sci., 2014, 292: 190-196.
6. Abdallah M, Rhodanine. Azosulpha drugs as corrosion inhibitors for corrosion of 304 stainless steel in hydrochloric acid solution. Corros Sci., 2002, 44: 717- 728.
7. Obi-Egbedi. NO, Obot, IB , Eseola, AO. Synthesis, characterization and corrosion inhibition efficiency of 2-(6-methylpyridine-2yl)-1H-imadazole [4,5-f] [1,10] phenanthroline on mild steel in sulphuric acid. Arabian J Chem., 2014, 7: 197-207.
8. Adnan sultan Abdul-Nabi, Ekhlas Qanber Jasim. Synthesis, Characterization and study of some tetrazole compounds as new corrosion inhibitors for C-steel in 0.5M HCl solution. Inter J Engg Res., 201, 3(10): 613-617.
9. Pearson RG. Absolute electronegativity and hardness: application to inorganic chemistry. Inorg Chem., 1988, 27: 734-740.
10. Obi-Egbedi NO, Essien KE, Obot IB, Ebenso EE. 1,2-Diaminoanthraquinone as corrosion inhibiotor for mild steel in Hydrochloric acid: weight loss and quantum chemical study. Int J Electrochem Sci., 2011, 6: 913-930.
11. Mahendra Yadav, Laldeep Gope, Tarun Kanti Sakar. Synthesized amino acid compounds as eco-friendly corrosion inhibitors for mild steel in hydrochloric acid solution: electrochemical and quantum studies. Res Chem Intermed., 2015, DOI10.1007/s11164-015-2172-5: 1.
12. Zhang F, Tang Y, Cao Z, Jing W, Wu Z, Chend Y. Performance and theoretical study on corrosion inhibition of 2-(4-pyridine)-benzimidezole for mild steel in hydrochloric acid. Corros Sci., 2012, 61: 1-9.
13. Ansari A, Znini M, Hamdani I, Majidi L, Bouyanzer A, Hammouti B. Experimental and theoretical investigations anti-corrosive properties of menthone on mild steel corrosion in hydrochloric acid. J Mater Environ Sci., 2014, 81-94.
14. Udhayakala P. A theoretical evaluation on quinoxaline derivatives as corrosion inhibitors on mild steel. Der Pharma Chemical., 2015, 7(11): 177-185.
15. Xia S, Qiu M, Yu L, Liu F, Zhao H. Molecular dynamic and density functional theory study on relationship between structure of imidazoline derivatives and inhibition performance. Corros. Sci., 2008, 50: 2012-2029.

*****